Available online at website: https://journal.bcrec.id/index.php/bcrec

Bulletin of Chemical Reaction Engineering & Catalysis, 19 (1) 2024, 99-107

Research Article

Bimetallic Ni-Fe Supported by Gadolinium Doped Ceria (GDC) Catalyst for CO_2 Methanation

Anis Kristiani[1,*], Kaoru Takeishi[2], Siti Nurul Aisyiyah Jenie[1], Himawan Tri Bayu Murti Petrus[3,4]

[1]*Research Centre for Chemistry, National Research and Innovation Agency (BRIN) Building 452 Kawasan Science and Technology B. J. Habibie Serpong, Tangerang Selatan, Banten, 15314, Indonesia.*
[2]*Shizuoka University, 3-5-1 Johoku, Hamamatsu-shi, Shizuoka-ken, 432-8561, Japan.*
[3]*Department of Chemical Engineering, Faculty of Engineering, Universitas Gadjah Mada, Jalan Grafika No 2, Yogyakarta, 55281, Indonesia.*
[4]*Unconventional Geo-Resources Research Center, Faculty of Engineering, UGM, Jl. Grafika No.2, Universitas Gadjah Mada, Yogyakarta, 55281, Indonesia.*

Received: 29th December 2023; Revised: 30th January 2024; Accepted: 31st January 2024
Available online: 5th February 2024; Published regularly: April 2024

Abstract

CO_2 conversion into fuels and high value-added chemical feedstocks, such as methane, has gained novel interest as a crucial process for further manufacturing multi-carbon products. Methane, CH_4, becomes a promising alternative for environmental and energy supply issues. Nickel-based catalysts were found to be very active and selective for CH_4 production. The use of promoter and support material to develop high activity, high selectivity, and durable catalysts for CO_2 methanation at low temperature is a challenge. Gadolinium-Doped Ceria (GDC) has been known as material for Solid Oxide Fuel Cell (SOFC) and Solid Oxide Electrolysis Cell (SOEC) due to higher ionic conductivity and lower operating temperatures. However, few researches have been done regarding to CO_2 methanation over GDC as catalyst support so far. In this present work, CO_2 methanation was investigated over bimetallic Ni-Fe catalyst supported by GDC. The results showed that CH_4 production rate by using Ni-Fe/GDC catalyst was higher than that of GDC at all reaction temperatures carried on. Ni-Fe/GDC showed remarkable CH_4 production rate as of 17.73 mmol.g_{cat}^{-1}.h^{-1} at 280 °C. No catalytic activity was produced by GDC catalyst only. The highest CO_2 conversion (46.50%) was observed at 280 °C, with almost 100% selectivity to CH_4. The turnover frequency (TOF) value of Ni-Fe/GDC (4529.32 h^{-1}) was the highest than that of Ni and common CO_2 methanation catalyst, Ni/Al_2O_3 catalysts at 280 °C, further displaying the outstanding low-temperature catalytic activity.

Keywords: Carbon dioxide; Catalyst; CO_2 Methanation; Gadolinium-Doped Ceria; Nickel-Iron Catalyst

How to Cite: A. Kristiani, K. Takeishi, S.N.A. Jenie, H.T.B.M. Petrus (2024). Bimetallic Ni-Fe Supported by Gadolinium Doped Ceria (GDC) Catalyst for CO_2 Methanation. *Bulletin of Chemical Reaction Engineering & Catalysis*, 19 (1), 99-107 (doi: 10.9767/bcrec.20108)

Permalink/DOI: https://doi.org/10.9767/bcrec.20108

1. Introduction

Global carbon dioxide emissions increased by 40% from 2000 to 2019, reaching a record high of 36.3 billion tons in 2021, contributing to global warming, the greenhouse effect, and severe environmental pollution [1,2]. Therefore, it is urgent to find a solution to reduce significantly the content of CO_2 in the atmosphere. Compared with the conventional CO_2 capture and storage (CCS) technologies, CO_2 capture, utilization, and storage (CCUS) technologies catalytically convert CO_2 into high value-added chemical feedstocks or fuels, such as CH_4, CH_3OH, and C_2H_5OH, which is critical to environmental protection and energy supply [3,4] . Compared with the conversion of CO_2 into other value-added chemicals, the CO_2

* Corresponding Author.
Email: anis.kristiani@brin.go.id (A. Kristiani);
Telp: +62-21-7560929, Fax: +62-21-7560546

methanation reaction rate is faster, the reaction conditions are milder, and can be carried out under atmospheric pressure [5].

$$CO_2\ (g) + 4H_2\ (g) \rightarrow CH_4\ (g) + 2H_2O\ (l)$$
$$\Delta H = -164 kJ/mol\ [6]$$

The hydrogenated product, CH_4, is available as a fuel and chemical feedstock for further manufacturing of multi-carbon products [7]. Carbon dioxide is a greenhouse gas that is abundantly found in the atmosphere. Utilizing carbon dioxide to produce methane would not only reduce the concentration of greenhouse gas in the atmosphere but would also be able to partially fulfill the energy demand [8,9].

The key to the highly effective conversion of CO_2 to CH_4 is the application of high-performance catalysts. Many different metals mainly in groups 8–10 such as Ni, Pd, Pt, Co, Rh, Fe, and Ru have been reported as active metals for fixed bed CO_2 methanation based on CO_2 conversion and CH_4 selectivity as summarized below [10,11]:
Activity to methanation: Ru > Rh > Ni > Fe > Co > Os > Pt > Ir > Mo > Pd > Ag > Au
Selectivity for methane: Pd > Pt > Ir > Ni > Rh > Co > Fe > Ru > Mo > Ag > Au

Among these catalysts, Ni-based catalysts are the most commonly CO_2 methanation catalysts due to their low price, abundant reserves, high CO_2 conversion, and CH_4 selectivity [5,12–14]. The activity of Ni-based catalysts is highly dependent on the natural character of the supports, which mainly affects the ability to adsorb and activate CO_2, the particle size of metal, the reducibility of metal phase, the interactions between metal and support, and the reaction mechanism [15,16]. Therefore, the choosing of support material to improve the activity and long-time stability of Ni-based catalysts is still a challenge [7,12].

Methanation catalysts can be used as a monometallic and multimetallic catalyst supported on various oxide, such as: TiO_2, SiO_2, γ-Al_2O_3, Y_2O_3, ZrO_2, YSZ, and CeO_2, and highly organized framework materials [8,12,17–19]. It is well-known that conventional Ni-based catalysts showed high catalytic activity at the high reaction temperature, low dispersion and reducibility, as well as nanoparticle sintering [14]. To overcome this drawback, addition of second transition metal (*e.g.*, Fe, Co) or a noble metal (*e.g.*, Ru, Rh, Pt, Pd and Re) has been reported to enhance the catalytic activity and stability of Ni-based catalysts for methanation reaction by improving the dispersion of active metal through Ni-M (metal) alloy formation and adjusting the interaction between Ni and the support [13,14]. It was also reported that NiFe alloys are active and stable catalysts for dry reforming of methane, since Fe can promote carbon gasification and significantly reduce coking through an intricate dealloying and realloying mechanism [14].

Catalysts $16Ni_xFe/Al_2O_3$ (x is 0, 1, 2, 4, 6, 8 prepared by incipient wetness impregnation method and applied for the production of synthetic natural gas (SNG) from CO hydrogenation in slurry-bed reactor were studied by Meng *et al.* [20]. It was found that the introduction of iron improved the catalytic performance of low-temperature CO methanation due to the formation of Ni-Fe alloy. G. De Piano *et al.* investigated the effect of Fe content in Ni-Fe bimetallic catalysts supported on $Ce_{0.8}Zr_{0.2}O_2$ (CZ) and SiO_2 (S) for CO_2 methanation. Bimetallic $N_{7.5}F_{2.5}$/CZ showed high activity stability during 30 h and no absence of carbon deposition after long-term treatment as well as no evidence of Ni sintering/decoration [21].

GDC has been utilized for catalytic applications due to their properties. Several its good properties are it has mixed ionic electronic conductivity under a reducing atmosphere, a sufficient ionic conductivity between 500 and 700 °C, and a good catalytic activity in CO_2 hydrogenation [22]. However, few research has been done regarding to CO_2 methanation over GDC as catalyst supports so far. A study of CO_2 methanation using nickel supported on GDC as catalyst at atmospheric pressure varying reaction temperature (300-600 °C) and space velocity (GHSV = 10,000 – 50,000 h^{-1}) was reported by Vita *et al.* [23]. Ni/GDC catalysts with different Ni content (15-50 wt%) were synthesized by the solution combustion synthesis and the result showed the catalytic performance increased by increasing the Ni content due to enhanced metal-to-support interaction, basicity and oxygen vacancies. Excellent stability was observed over 200 h of time-on-stream. Study on bimetallic catalysts for CO_2 methanation was investigated over Ni and Ni-Fe catalysts supported on GDC in the temperature range 200-400 °C [24]. The result showed that both CO_2 and H_2 conversion decreased in the order Ni/GDC > Ni_3Fe_1/GDC> Ni_1Fe_1/GDC > Ni_1Fe_3/GDC. No catalytic activity was produced by Fe/GDC only. Maximum CO_2 conversion (>90%) was observed at 400 °C, with almost 100% selectivity to CH_4. The superior activity of monometallic Ni/GDC and bimetallic Ni-Fe/GDC catalysts was ascribed to the presence of surface oxygen vacancies induced by the GDC support, an enhanced basicity of the Ni-rich samples, as well as to the ability of the Ni-GDC to interact with CO_2. Similar study was also conducted by Frontera *et al.* The nickel-iron supported on GDC have been tailored for simultaneous methanation of carbon monoxide and carbon dioxide. It was found that NiFe/GDC catalyst exhibited its highest carbon conversion at 500 °C [6].

Regarding the literature review, a few researchers focused on the use of bimetallic nickel-

iron supported on GDC for low-temperature CO_2 methanation. There have been limited studies concerned on catalyst with high activity at low temperature and enhanced anti-sintering and anti-coking properties for CO_2 methanation. Therefore, this research intends to low-temperature of CO_2 methanation. The objective of this research is to investigate the catalytic performance of Ni-Fe/GDC catalyst for low-temperature CO_2 methanation.

2. Materials and Methods

2.1 Materials

Catalyst precursors used are NiO (Sumitomo Metal Mining Co.), GDC (Anan Kasei Co.), and Fe_2O_3 (Sumitomo Metal Mining Co.). Reactant gases used are hydrogen, argon, and carbon dioxide. Each of their purity are 99.999%, 99.995%, and 99.95%, respectively.

2.2. Catalyst Preparation

Ni-Fe/GDC catalyst was prepared by physical mixture method. Briefly, NiO was mixed by Fe_2O_3, and GDC as support (Ni: Fe: GDC ratio is 30: 30: 40 wt.%) under dry condition. Afterwards, the obtained solid was calcined at high temperature of 1400 ºC for 2 h. Prior the reaction, the Ni-Fe/GDC catalyst powder was reduced in situ with 10 ml/min H_2 flow at various temperature in the range of 500 ºC until 700 ºC for 2 h.

2.3. Catalyst Characterization

Powder X-ray diffraction patterns were collected using a Rigaku RINT 2000 equipped with a Cu Kα (λ=1.5418 Å) source and the Brag-Brentano θ-θ configuration in the 10-90° 2θ range, with 0.05° step size and 2 s acquisition time. The surface area of the catalysts was measured by N_2 adsorption desorption isotherms at 77 K using a Micromeritics ASAP 2010 apparatus. Before measurement, the catalysts were degassed at 300 ºC in N_2 for 5 h. The surface area was calculated by the Brunauer-Emmet-Teller (BET) method in the equilibrium pressure range $0.05 < P/P° < 0.3$. H_2-temperature programmed reduction (H_2-TPR) of the samples were performed using BEL MULTI-TASK-TPD. Analysis was carried out on 300 mg of sample, heating from 50 to 800 ºC at a heating rate of 5 °C/min with 10% H_2 flow rate of 5 ml/min and holding at the final temperature for 5 h. The H_2 consumption was measured by a mass spectrometer (MS). CO_2-temperature programmed desorption (CO_2-TPD) of the samples were performed using BEL MULTI-TASK-TPD. Analysis was carried out on 1000 mg of sample, heating from room temperature to 500 ºC at a heating rate of 5 °C/min with helium gas flow rate of 50 mL/min for 30 min. After the cleaning with He gas, the samples were cooled to 50 ºC, switched in CO_2 and saturated down at 50 ºC. Then, the samples were purged again with He. The CO_2 consumption of it was measured by an MS detector with heating from 50 ºC to 500 ºC.

2.4. Catalytic Activity Tests

The performance of the catalysts was evaluated for CO_2 methanation. Prior to the activity tests, 1.00 g of catalyst was placed inside a stainless steel fixed bed reactor (inner diameter: 9.0 mm), with quartz wool at both ends, and reduced in situ with 10 mL/min H_2 flow, increasing the temperature from room temperature up to 700 °C and isothermally kept at this temperature for 2 h. Different reduction temperatures were employed to determine the effect of reduction temperature. Afterwards, the feed mixture was flowed through the reactor. The reactions were performed in a fixed bed reactor operating at atmospheric pressure by means of gaseous mixtures of $H_2/CO_2/Ar$ with different volumetric ratios in a temperature range 200-320 °C with 40 °C increments and GHSV 18,750 h^{-1}. Each temperature step was maintained for 60 min.

The performance of the catalysts was evaluated in terms of CO_2 conversion, CH_4 selectivity, CH_4 production rate, and TOF. These values were calculated by the equations given as Equation (1), (2), (3), and (4), respectively.

$$X\,CO_2 = \frac{N_{CO_2\ in} - N_{CO_2\ out}}{N_{CO_2\ in}} \times 100 \quad (1)$$

where, $X\ CO_2$ is CO_2 conversion (%), CO_2 in is molar amount of CO_2 based on (mol) and CO_2 out is CO_2 molar amount of outlet (mol).

$$S\,CH_4 = \frac{N_{CH_4}}{N_{total}} \times 100 \quad (2)$$

where, S CH_4 is CH_4 selectivity (%), N CH_4 is molar amount of formed CH_4 (mol/g/h) and N total is molar amount of the whole formed carbon compounds (mol/g/h).

$$CH_4\ pro = \frac{N_{CH_4}}{1{,}000{,}000} \quad (3)$$

where $CH_4\ pro$ is CH_4 production rate (mmol/g/h), N CH_4 is molar amount of formed CH_4 (mol/g/h). Turnover frequency (TOF) for methane production is calculated as follows:

$$TOF(s^{-1}) = \frac{MPR\ (mmol.g\ cat^{-1}h^{-1})}{AAS\ (mmol.g\ cat^{-1})} \quad (4)$$

MPR denotes methane production rate (mmol.gcat^{-1}.h^{-1})), and AAS expresses amount of active sites (Ni amount on the catalyst surface) (mmol.gcat^{-1}). The amount of active sites (Ni amount on the catalyst surface) of each catalyst was measured by CO pulse titration and H_2 pulse titration at 50 ºC using BEL MULTI-TASK-TPD.

2.4 Product Analysis

The products were analyzed by two online gas chromatographs (Shimadzu GC-14B) consisted of two detectors, thermal conductivity detector (TCD) and flame ionization detector (FID) in series. Each of GCs have a Molecular Sieve 5A and a Porapak T columns, for analyses of gases and liquids including CO_2, respectively.

3. Results and Discussion

3.1 Characterization of the Catalysts

The specific surface area of the catalyst samples was calculated from their respective N_2 adsorption isotherms as shown in Table 1. GDC showed higher specific surface area compared to Ni-Fe/GDC. It indicated that the deposition of bimetallic Ni-Fe changed the textural properties of the GDC support as shown by BET surface areas (0.69 $m^2.g^{-1}$) that are lower than GDC support (13.2 $m^2.g^{-1}$). It is also worth noting that the specific surface area of Ni-Fe/GDC catalyst decreased in comparison with GDC support after introducing Ni and Fe species, indicating that Ni and Fe nanoparticles successfully entered the interior of GDC support and blocked the pore during the preparation [7]. The specific surface area of Ni-Fe/GDC catalysts after reduced at temperature of 700 °C tend to remain stable in the range of 0.66 $m^2.g^{-1}$. It indicated that GDC as support contributed to maintain the specific surface area and minimize the sintering effect of Ni and Fe particles in Ni-Fe/GDC at high reduction temperature.

The XRD analysis was carried out to find out the presence of the metallic states of active metals. Figure 1 shows the XRD patterns of reduced Ni, GDC and Ni-Fe/GDC catalysts. Reduced Ni catalyst exhibited the characteristic peaks of Ni at 2θ angle of 44.3°, and 51.8°, indicating that NiO was reduced to metallic Ni°. Both of GDC and Ni-Fe/GDC catalysts showed the existence of cubic fluorite structure of GDC support at 2θ = 28°, 33°, 47°, 56°, 59°, 69°, 76° and 79° as shown in Figure 1. The new diffraction peaks due to the interaction between iron and nickel in Ni-Fe/GDC catalysts were observed at 2θ = 44.35° and 51.65° can be assigned to the (111) and (200) of cubic phase of $FeNi_3$ species (JCPDS card No. 65-3244). It revealed the formation of Ni-Fe alloy. Combined with the catalytic performance described in Figure 4-6, the results suggested that the formation of Ni-Fe alloy plays an important factor for CO_2 methanation reaction over the Ni species that existed in the catalysts [20,25].

Metal-support interactions and metal reducibility are assessed by H_2-TPR (Figure 2). Based on the H_2-TPR characterizations, most of NiO can be reduced to Ni at the reduction

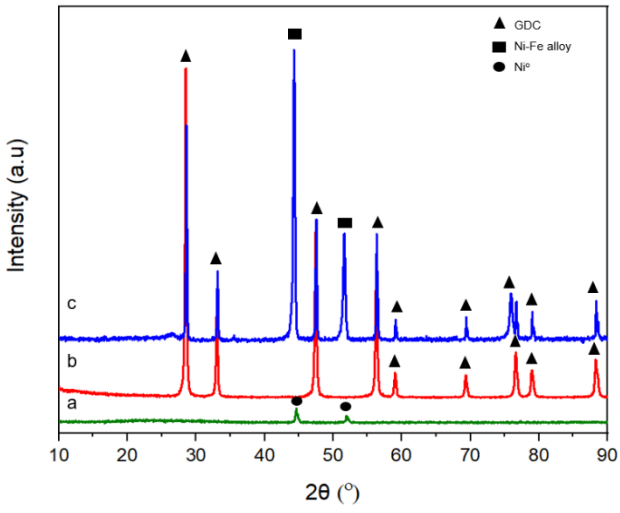

Figure 1. XRD patterns of reduced catalysts (a) Ni, (b) GDC, (c) Ni-Fe/GDC.

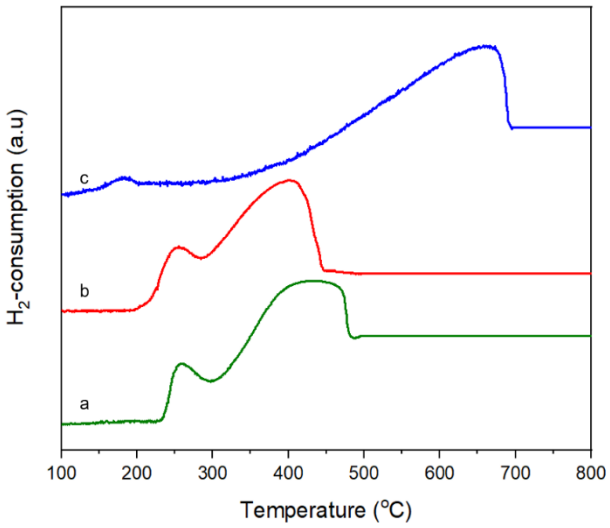

Figure 2. H_2-TPR profile of reduced catalysts (a) Ni, (b) GDC, (c) Ni-Fe/GDC.

Table 1. Textural properties of GDC support and Ni-Fe/GDC catalysts.

Catalyst	Specific surface area ($m^2.g^{-1}$)	Pore volume ($cm^3.g^{-1}$)	Pore size (nm)
GDC as prepared	13.2	0.044	12.4
GDC 800°C -2h-red	4.23	0.011	11.5
Ni-Fe/GDC as prepared	0.69	0.002	10.9
Ni-Fe/GDC 700°C -2h-red	0.66	0.001	10.5

temperature of 500 °C. Generally, bulk NiO is reduced at about 300 °C [7,18]. The peaks at higher temperatures suggested different level of interactions between Ni species and the support [18,23,26]. From Figure 2, it can be seen that the peaks at 340–695 °C in the Ni-Fe/GDC catalysts were attributed to the reduction of dispersed NiO that strongly interacted with the GDC support.

To determine the surface basic sites, CO_2-TPD measurements were performed for all reduced catalysts (Figure 3). There are three CO_2 desorption regions depending on the desorption temperature, corresponding to weak basic sites (< 200 °C), moderate basic sites (200–400 °C) and strong basic sites (> 400 °C), respectively [27]. GDC and Ni-Fe/GDC reduced catalyst display mainly a high density of weak basic sites. As can be seen in Figure 3, Ni reduced catalyst shows weak and medium basic sites. Li *et al.* [2] proposed that CO_2 was adsorbed by surface hydroxyl groups with weak basic sites to generate the reactive carbonate species that further reacted with dissociated H atoms to produce CH_4. Whereas, moderate basic sites promoted the formation of reactive bidentate carbonates and followed by hydrogenation to CH_4. However, the strong basic sites did not provide to CO_2 methanation reaction [7,21]. The use of GDC support plays a pivotal role in reaction, enhancing the basicity of the Ni-Fe/GDC catalyst and improving the dissociation of carbon oxide species adsorbed on Ni sites [28].

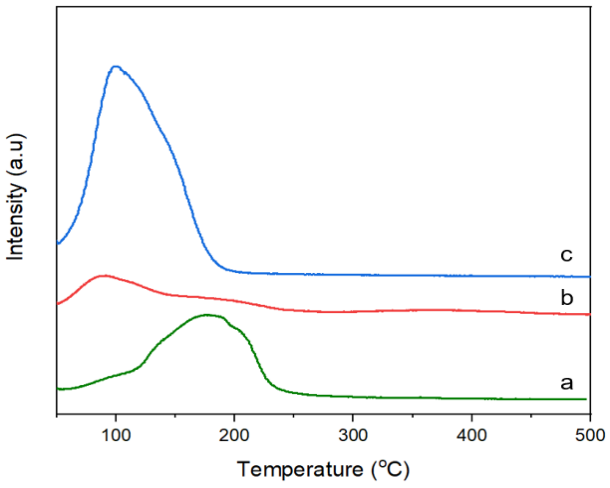

Figure 3. CO_2-TPD profile of reduced catalysts (a) Ni, (b) GDC, (c) Ni-Fe/GDC.

3.2 Catalytic Activity Results of CO_2 Methanation

To study the effect of feed ratios, several test runs were performed at reaction temperatures of 200 to 320 °C with a total feed flow rate of 100 mL/min. CO_2 conversion, CH_4 selectivity and CH_4 production rate results are displayed in Figures 4-6. It can be seen that almost all of the catalysts are not active below 200 °C. Different reduction temperatures were chosen to determine the effect on the performance of catalysts for CO_2 hydrogenation reaction at the feed gas ratio $H_2/CO_2 = 4/1$. The higher reduction temperature of Ni-Fe/GDC catalysts improved the performance of catalysts on methanation reaction. Ni-Fe/GDC catalysts produced higher CO_2 conversion and CH_4 selectivity compared with GDC and Ni catalyst. The best performance of the catalysts was located at the temperature of 280 °C. The CO_2 conversion and CH_4 selectivity are decreased at higher reaction temperature, due to the enhancement of CO Boudouard reaction, reverse methane reforming reaction by CO_2, and water-gas shift reaction [18,25]. This result was better than previous research using Ni-Fe/GDC catalysts that performed lower CO_2 methanation activity (XCO_2 < 20%) at reaction temperature under 300 °C [6].

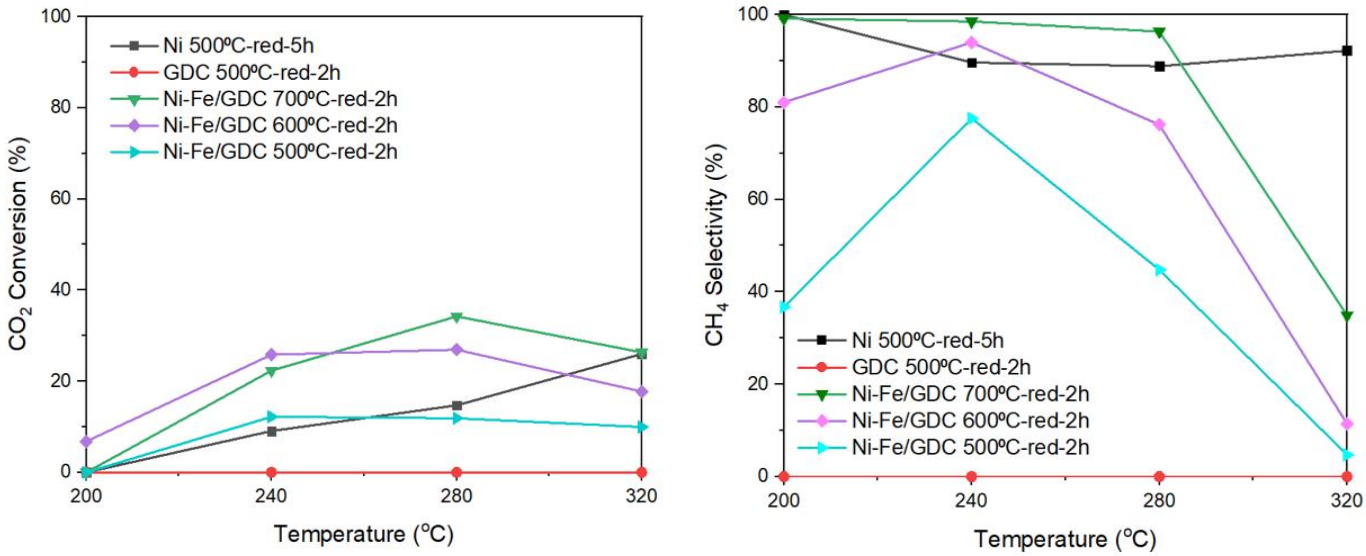

Figure 4. Catalytic performance of Ni, GDC and Ni-Fe supported by GDC at various reduction

As shown in Figure 5, methanation activity of nickel-iron supported by GDC was better than those on Ni unsupported and GC support only. GDC catalyst performed poor methanation activity at all reaction temperatures conducted. Meanwhile, Ni-Fe/GDC catalysts performed higher CH_4 production rate per catalyst weight compared with GDC catalyst in all reaction temperatures carried on. It suggested that the existence of GDC minimized the sintering of nickel and iron metal particle at higher reaction temperature and contributed to the catalytic activity of Ni-Fe/GDC catalyst for methanation at higher reaction temperature. Compared with Ni catalyst, Ni-Fe/GDC catalysts also exhibited higher CH_4 production rate at reaction temperature of 280 °C. It confirms that the addition of Fe in Ni-Fe/GDC catalyst could facilitate the dispersion of Ni particles and enhance the activity of catalyst at low temperatures. CH_4 production rates of Ni-Fe/GDC catalysts tend to increase by the increase of reduction temperature in the following order: 500 °C < 600 °C < 700 °C. The Ni-Fe/GDC catalyst reduced at 700 °C for 2 h produced the highest CH_4 production rates of 17.6 mmol.gcat^{-1}.h^{-1} at reaction temperature of 280 °C. It was slightly higher compared to Ni-Fe/GDC catalyst reduced at 600 °C for 2 h which produced CH_4 production rates of 17.2 mmol.gcat^{-1}.h^{-1} at 280 °C.

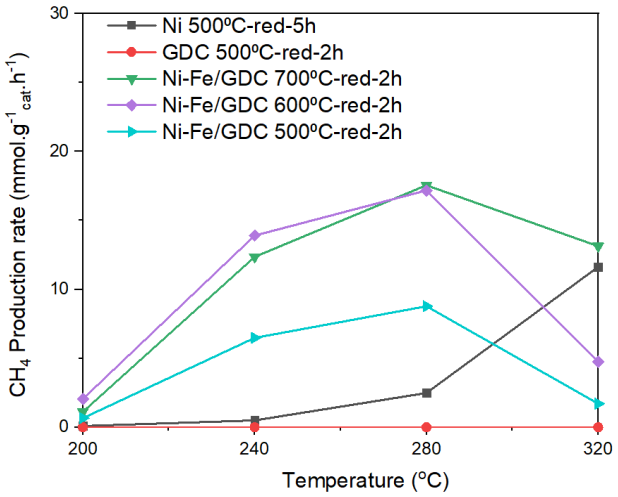

Figure 5. CH_4 production rate per catalyst weight.

Ni/Al_2O_3 catalysts are well-known as common catalysts for methanation due to the high specific surface area of Al_2O_3 [18,29]. Figure 6 shows the TOF for methane (methane produced per nickel site per second) production by CO_2 methanation on nickel-iron supported by GDC compared with nickel supported by Al_2O_3, and nickel unsupported. From Figure 6, we find out that the TOF for methane production by CO_2 methanation on Ni-Fe/GDC catalyst was higher than Ni/Al_2O_3 and Ni catalyst due to the existence of GDC support and the addition of Fe_2O_3. The use of GDC as supports contribute to the higher catalytic activity compared with Al_2O_3 due to the increase of oxygen vacancies by the addition of ceria to rare earth oxides (Gd_2O_3) forms a solid Ce^{4+} oxide solution with CeO_2 that contains mainly cations. This presence of surface oxygen vacancies enhances the surface basicity of pure CeO_2 and promotes CO_2 methanation [24,30]. The addition

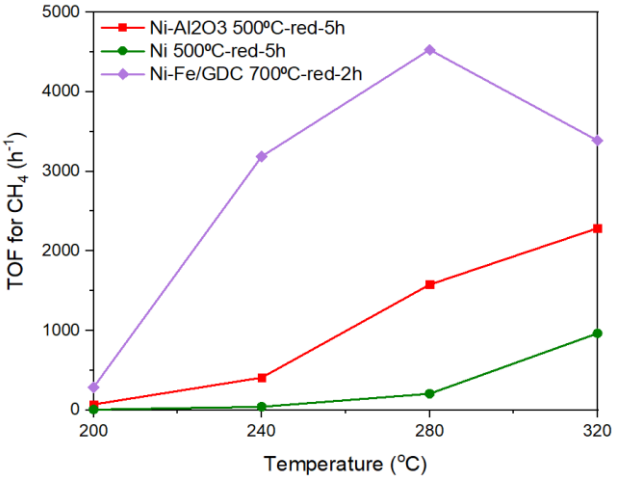

Figure 6. TOF of Ni, Ni-Fe/GDC, and Ni/Al_2O_3 catalyst.

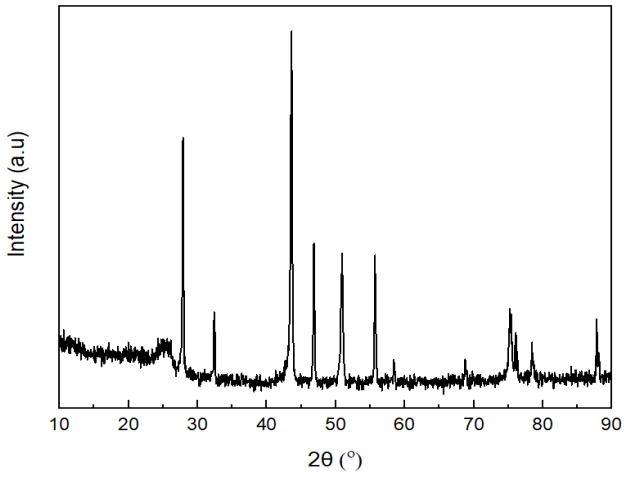

Figure 7. XRD patterns of Ni-Fe/GDC spent catalyst.

Table 2. CO_2 conversion (%), CH_4 selectivity (%) and TOF values (s^{-1}) for different Ni-Fe based catalysts.

Catalyst	*X* CO_2 (%)	*S* CH_4(%)	TOF (s^{-1})	Reference
Ni-Fe/$Ce_{0.8}Zr_{0.2}O_2$ (CZ)	24.80 at 300 °C	90 at 300 °C	0.050	[21]
Ni-Fe/S	12.1 at 300 °C	35 at 300 °C	0.268	[21]
Ni-Fe/GDC 700 °C-2h-red	34.23 at 280 °C	96 at 280 °C	1.258	This work

of Fe_2O_3 promotes CO_2 hydrogenation compared with the Ni catalysts without GDC or/and Fe_2O_3 by electronic modification of Ni, forming Ni-Fe alloy nanoparticles [21,31,32]. The highest TOF (4529.32 h^{-1}) was produced by Ni-Fe/GDC catalyst at reaction temperature of 280 ºC. The best result obtained at 280 ºC for Ni-Fe/GDC catalyst is superior to previously reported Ni-Fe based catalyst as shown in Table 2 [21].

Deactivation of a metal catalyst can occur due to several factors, such as adsorption of impurities from the feed or product streams, coke deposition on the catalyst surface, oxidation of metal, metallic surface area reduction from sintering or leaching, and a drop in surface area from pore blockage [33]. XRD analysis was performed on Ni-Fe/GDC spent catalyst. Metal-supported spent catalysts usually show the peaks for graphitic coke formation at $2\theta = 62°$ and atomic coke formation at $2\theta = 30°$, respectively [34]. From the XRD pattern in Figure 7, no such peak was found for Ni-Fe/GDC spent catalysts.

4. Conclusions

In summary, we have studied CO_2 methanation activity over bimetallic Ni-Fe supported by GDC catalyst. Ni-Fe/GDC catalyst exhibited the highest CO_2 conversion (46.5%) at 280 ºC, with almost 100% selectivity to CH_4 under a GHSV of 18,750 h^{-1} at $H_2/CO_2 = 4$. The TOF value of Ni-Fe/GDC (4529 h^{-1}) was the highest than that of Ni and common CO_2 methanation catalyst, Ni/Al_2O_3 catalysts at 280 ºC, further displaying the outstanding low-temperature catalytic activity.

Acknowledgments

The authors would like to acknowledge funding from Japan Science and Technology Agency-Core Research for Evolutional Science and Technology (JST-CREST) through a project entitled “Development of Innovative Technology for Energy-Carrier Synthesis using Novel Solid Oxide Electrolysis Cell (JPMJCR1343)”.

Credit Author Statement

A. Kristiani: Experimental work, Data analysis, Writing-Original draft preparation, Writing-Review and Editing; *K.* Takeishi: Conceptualization, Methodology, Supervision, Writing-Review, Funding acquisition; *S.N.A. Jenie*: Writing-Review, Funding acquisition; *H.B.T.M. Petrus*: Writing-Review, Funding acquisition. All authors have read and agreed to the published version of the manuscript.

References

[1] Tong, D., Zhang, Q., Zheng, Y., Caldeira, K., Shearer, C., Hong, C., Qin, Y., Davis, S.J. (2019). Committed emissions from existing energy infrastructure jeopardize 1.5 °C climate target. *Nature*, 572(7769), 373–377. DOI: 10.1038/s41586-019-1364-3.

[2] Li, Y., Men, Y., Liu, S., Wang, J., Wang, K., Tang, Y., An, W., Pan, X., Li, L. (2021). Remarkably efficient and stable Ni/Y_2O_3 catalysts for CO_2 methanation: Effect of citric acid addition. *Applied Catalysis B: Environmental*, 293, 120206. DOI: 10.1016/j.apcatb.2021.120206.

[3] Quindimil, A., De-La-Torre, U., Pereda-Ayo, B., González-Marcos, J.A., González-Velasco, J.R. (2018). Ni catalysts with La as promoter supported over Y- and BETA- zeolites for CO_2 methanation. *Applied Catalysis B: Environmental*, 238, 393–403. DOI: 10.1016/j.apcatb.2018.07.034.

[4] Li, M.M.J., Chen, C., Ayvall, T., Suo, H., Zheng, J., Teixeira, I.F., Ye, L., Zou, H., O'Hare, D., Tsang, S.C.E. (2018). CO_2 Hydrogenation to Methanol over Catalysts Derived from Single Cationic Layer CuZnGa LDH Precursors. *ACS Catalysis*, 8 (5), 4390–4401. DOI: 10.1021/acscatal.8b00474.

[5] Li, L., Zeng, W., Song, M., Wu, X., Li, G., Hu, C. (2022). Research Progress and Reaction Mechanism of CO_2 Methanation over Ni-Based Catalysts at Low Temperature: A Review. *Catalysts*, 12 (2), 1–24. DOI: 10.3390/catal12020244.

[6] Frontera, P., Macario, A., Malara, A., Antonucci, V., Modafferi, V., Antonucci, P.L. (2020). Simultaneous methanation of carbon oxides on nickel-iron catalysts supported on ceria-doped gadolinia. *Catalysis Today*, 357, 565–572. DOI: 10.1016/j.cattod.2019.05.065.

[7] Han, F., Liu, Q., Li, D., Ouyang, J. (2023). An emerging and high-performance sepiolite-supported Ni catalyst for low-temperature CO2 methanation: The critical role of hydroxyl groups. *Journal of Environmental Chemical Engineering*, 11 (5), 110331. DOI: 10.1016/j.jece.2023.110331.

[8] Malara, A., Frontera, P., Antonucci, P., Macario, A. (2020). Smart recycling of carbon oxides: Current status of methanation reaction. *Current Opinion in Green and Sustainable Chemistry*, 26, 100376. DOI: 10.1016/j.cogsc.2020.100376.

[9] Fan, W.K., Tahir, M. (2021). Recent trends in developments of active metals and heterogenous materials for catalytic CO_2 hydrogenation to renewable methane: A review. *Journal of Environmental Chemical Engineering*, 9 (4), 105460. DOI: 10.1016/j.jece.2021.105460.

[10] Younas, M., Loong Kong, L., Bashir, M.J.K., Nadeem, H., Shehzad, A., Sethupathi, S. (2016). Recent Advancements, Fundamental Challenges, and Opportunities in Catalytic Methanation of CO_2. *Energy & Fuels*, 30 (11), 8815–8831. DOI: 10.1021/acs.energyfuels.6b01723.

[11] Rönsch, S., Schneider, J., Matthischke, S., Schlüter, M., Götz, M., Lefebvre, J., Prabhakaran, P., Bajohr, S. (2016). Review on methanation – From fundamentals to current projects. *Fuel*, 166, 276–296. DOI: https://doi.org/10.1016/j.fuel.2015.10.111.

[12] Italiano, C., Llorca, J., Pino, L., Ferraro, M., Antonucci, V., Vita, A. (2020). CO and CO_2 methanation over Ni catalysts supported on CeO_2, Al_2O_3 and Y_2O_3 oxides. *Applied Catalysis B: Environmental*, 264, 118494. DOI: 10.1016/j.apcatb.2019.118494.

[13] Lv, C., Xu, L., Chen, M., Cui, Y., Wen, X., Li, Y., Wu, C., Yang, B., Miao, Z., Hu, X., Shou, Q. (2020). Recent Progresses in Constructing the Highly Efficient Ni Based Catalysts With Advanced Low-Temperature Activity Toward CO_2 Methanation. *Frontiers in Chemistry*, 8, 269. DOI: 10.3389/fchem.2020.00269.

[14] Tsiotsias, A.I., Charisiou, N.D., Yentekakis, I. V, Goula, M.A. (2021). Bimetallic Ni-Based Catalysts for CO_2 Methanation: A Review. *Nanomaterials*, 11 (1), 28. DOI: 10.3390/nano11010028.

[15] Marconi, E., Tuti, S., Luisetto, I. (2019). Structure-sensitivity of CO_2 methanation over nanostructured Ni supported on CeO_2 nanorods. *Catalysts*, 9(4), 375. DOI: 10.3390/catal9040375.

[16] Winter, L.R., Gomez, E., Yan, B., Yao, S., Chen, J.G. (2018). Tuning Ni-catalyzed CO_2 hydrogenation selectivity via Ni-ceria support interactions and Ni-Fe bimetallic formation. *Applied Catalysis B: Environmental*, 224, 442–450. DOI: 10.1016/j.apcatb.2017.10.036.

[17] Lee, W.J., Li, C., Prajitno, H., Yoo, J., Patel, J., Yang, Y., Lim, S. (2021). Recent trend in thermal catalytic low temperature CO_2 methanation: A critical review. *Catalysis Today*, 368, 2–19. DOI: 10.1016/j.cattod.2020.02.017.

[18] Kristiani, A., Takeishi, K. (2022). CO_2 methanation over nickel-based catalyst supported on yttria-stabilized zirconia. *Catalysis Communications*, 165, 106435. DOI: 10.1016/j.catcom.2022.106435.

[19] Hu, F., Jin, C., Lim, K.H., Li, C., Song, G., Bella, Wang, T., Ye, R., Lu, Z.H., Feng, G., Zhang, R., Kawi, S. (2023). Promoting hydrogen spillover of NiFe/CeO_2 catalyst with plasma-treatment for CO_2 methanation. *Fuel Processing Technology*, 250, 107873. DOI: 10.1016/j.fuproc.2023.107873.

[20] Meng, F., Zhong, P., Li, Z., Cui, X., Zheng, H. (2014). Surface structure and catalytic performance of Ni-Fe catalyst for low-temperature CO hydrogenation. *Journal of Chemistry*, 2014, 534842. DOI: 10.1155/2014/534842.

[21] De Piano, G., Gamboa, J.J.A., Condó, A.M., Bengió, S., Gennari, F.C. (2022). Bimetallic Ni-Fe catalysts for methanation of CO_2: Effect of the support nature and reducibility. *Applied Catalysis A: General*, 634, 118540. DOI: 10.1016/j.apcata.2022.118540.

[22] Naseer, A., Hussain, M., Shakir, I., Abbas, Q., Yilmaz, D., Zahra, M., Raza, R. (2020). The robust catalysts (Ni1−x–Mox/doped ceria and Zn1−x–Mox/doped ceria, x = 0.1 and 0.3) for efficient natural gas reforming in solid oxide fuel cells. *Electrochimica Acta*, 361, 137033. DOI: 10.1016/j.electacta.2020.137033.

[23] Vita, A., Italiano, C., Pino, L., Frontera, P., Ferraro, M., Antonucci, V. (2018). Activity and stability of powder and monolith-coated Ni/GDC catalysts for CO_2 methanation. *Applied Catalysis B: Environmental*, 226, 384–395. DOI: 10.1016/j.apcatb.2017.12.078.

[24] Frontera, P., Macario, A., Monforte, G., Bonura, G., Ferraro, M., Dispenza, G., Antonucci, V., Aricò, A.S., Antonucci, P.L. (2017). The role of Gadolinia Doped Ceria support on the promotion of CO_2 methanation over Ni and Ni–Fe catalysts. *International Journal of Hydrogen Energy*, 42 (43), 26828–26842. DOI: 10.1016/j.ijhydene.2017.09.025.

[25] Cheng, C., Shen, D., Xiao, R., Wu, C. (2017). Methanation of syngas (H_2/CO) over the different Ni-based catalysts. *Fuel*, 189, 419–427. DOI: 10.1016/j.fuel.2016.10.122.

[26] Boukha, Z., Bermejo-López, A., De-La-Torre, U., González-Velasco, J.R. (2023). Behavior of nickel supported on calcium-enriched hydroxyapatite samples for CCU-methanation and ICCU-methanation processes. *Applied Catalysis B: Environmental*, 338, 122989. DOI: 10.1016/j.apcatb.2023.122989.

[27] He, F., Zhuang, J., Lu, B., Liu, X., Zhang, J., Gu, F., Zhu, M., Xu, J., Zhong, Z., Xu, G., Su, F. (2021). Ni-based catalysts derived from Ni-Zr-Al ternary hydrotalcites show outstanding catalytic properties for low-temperature CO2 methanation. *Applied Catalysis B: Environmental*, 293, 120218. DOI: 10.1016/j.apcatb.2021.120218.

[28] Frontera, P., Macario, A., Malara, A., Modafferi, V., Mascolo, M.C., Candamano, S., Crea, F., Antonucci, P. (2018). CO_2 and CO hydrogenation over Ni-supported materials. *Functional Materials Letters*, 11(5), 1–4. DOI: 10.1142/S1793604718500613.

[29] Weber, S., Abel, K.L., Zimmermann, R.T., Huang, X., Bremer, J., Rihko-Struckmann, L.K., Batey, D., Cipiccia, S., Titus, J., Poppitz, D., Kübel, C., Sundmacher, K., Gläser, R., Sheppard, T.L. (2020). Porosity and structure of hierarchically porous Ni/Al_2O_3 catalysts for CO_2 methanation. *Catalysts*, 10(12), 1–22. DOI: 10.3390/catal10121471.

[30] Sun, Q., Fu, Z., Yang, Z. (2018). Effects of rare-earth doping on the ionic conduction of CeO_2 in solid oxide fuel cells. *Ceramics International*, 44 (4), 3707–3711. DOI: 10.1016/j.ceramint.2017.11.149.

[31] Burger, T., Augenstein, H.M.S., Hnyk, F., Döblinger, M., Köhler, K., Hinrichsen, O. (2020). Targeted Fe-Doping of Ni−Al Catalysts via the Surface Redox Reaction Technique for Unravelling its Promoter Effect in the CO2 Methanation Reaction. *ChemCatChem*, 12(2), 649–662. DOI: 10.1002/cctc.201901331.

[32] Serrer, M.A., Gaur, A., Jelic, J., Weber, S., Fritsch, C., Clark, A.H., Saraçi, E., Studt, F., Grunwaldt, J.D. (2020). Structural dynamics in Ni-Fe catalysts during CO_2 methanation-role of iron oxide clusters. *Catalysis Science and Technology*, 10(22), 7542–7554. DOI: 10.1039/d0cy01396j.

[33] Hossain, M.Z., Chowdhury, M.B.I., Alsharari, Q., Jhawar, A.K., Charpentier, P.A. (2017). Effect of mesoporosity of bimetallic Ni-Ru-Al_2O_3 catalysts for hydrogen production during supercritical water gasification of glucose. *Fuel Processing Technology*, 159, 55–66. DOI: 10.1016/j.fuproc.2017.01.013.

[34] Hossain, M.Z., Chowdhury, M.B.I., Jhawar, A.K., Xu, W.Z., Biesinger, M.C., Charpentier, P.A. (2018). Continuous Hydrothermal Decarboxylation of Fatty Acids and Their Derivatives into Liquid Hydrocarbons Using Mo/Al_2O_3 Catalyst. *ACS Omega*, 3(6), 7046–7060. DOI: 10.1021/acsomega.8b00562.